PHYSICS AND CHEMISTRY OF SOLID STATE
V. 25, No. 2 (2024) pp.235-244
Section: Physics

DOI: 10.15330/pcss.25.2.235-244

Vasyl Stefanyk Precarpathian National University

ФІЗИКА І ХІМІЯ ТВЕРДОГО ТІЛА
Т. 25, № 2 (2024) С. 235-244
Фізико-математичні науки

PACS: 78.67.Hc, 78.20.Ci, 71.15.-m.

ISSN 1729-4428 (Print)
ISSN 2309-8589 (Online)

V.B. Holskyi, R.Ya. Leshko, V.B. Brytan, Y.O. Uhryn, V.R. Karpiy

The Influence of Polarized Phonons on Interband Light Absorption in Spheroidal Quantum Dots of the CdS/SiO_2 Heterosystem

Department of physics and information systems, Drohobych Ivan Franko State Pedagogical University, Drohobych, Lviv region, Ukraine, hol.wit@gmail.com

The influence of confined phonons on the coefficient of interband absorption of polarized light as a function of its frequency has been investigated. A comparison was made between the obtained results and those obtained considering polarized phonons in a bulk crystal. The dependence of interband light absorption on the ellipsoid's axis ratio has been established. Calculations were performed for various temperatures and radii of the quantum dot in the CdS/SiO_2 heterostructure, shaped as an elongated spheroid.

Keywords: optical transitions, confined phonons, absorption coefficient, quantum dots.

Received 15 December 2023; Accepted 28 April 2024.

Introduction

The impact of quantum effects on the optical properties of semiconductor quantum dots (QDs) is a subject of intensive research in solid-state physics. The primary interest in these low-dimensional structures arises from their potential applications in optoelectronics. Current experimental and theoretical studies have extensively explored the energy levels of bound states in nanocrystals. However, the influence of phonons in QDs requires further investigation.

Due to their unique properties, QDs can be utilized in devices such as night vision equipment, solar cells, field-effect transistors, and light-emitting devices [1]. Optical devices in the mid-infrared range can be realized based on interband transitions of electrons (holes). Such transitions are actively studied both theoretically and experimentally [2-4]. The temperature dependencies of the energy difference between energy levels, chemical potential levels, and electron distribution among lower sublevels, affecting the interband absorption coefficient, have been explored in a study [5]. The absorption coefficient of QDs in the adiabatic approximation has been determined in another study [6], where the expression for the interaction of the electron-hole system with longitudinal optical phonons of a massive crystal was employed.

Research indicates that the shape of QDs significantly influences the energy spectrum of quasi-particles [7]. Experimental works highlight the difference in shape from spherical [8-10], which ultimately manifests in the optical properties of materials. However, most studies are devoted to spherically symmetric QDs due to their simpler solution. Linear and nonlinear absorption coefficients in QDs of spherical shape have been calculated in a study [2]. For nanocrystals in the form of a lens, the absorption coefficient of light has been calculated, considering impurities within the QDs [3]. Special attention is given to the ellipsoidal shape due to its closer correspondence with experimental dimensions of QDs [9].

The phonon spectrum in spheroidal QDs has been investigated in works [11-14]. In studies [11-12], interface optical phonons for QDs in the form of an elongated or flattened spheroid were examined in the dielectric continuum model, demonstrating a pronounced dependence of their spectrum on the nanocrystal's geometry. The Raman spectrum in QDs with a non-spherical shape was experimentally studied [13], proposing a theoretical model that showed good convergence. The polaron spectrum in spheroidal QDs was investigated in a study [14], where the phonon spectrum was considered using the variational method. It was shown that the polaron binding energy decreases with

an increase in the nanocrystal's radius, with the main contribution coming from LO phonons.

Analysis indicates the current relevance of studying the absorption coefficient in nanocrystals with shapes different from spherical, considering the phonon spectrum. Therefore, the aim of this work is to determine the dependence of the light absorption coefficient on the degree of elongation of the spheroid, taking into account confined phonons.

I. Quantum Dot Model

We consider a spheroidal-shaped quantum dot of a wide-bandgap semiconductor embedded in a semiconductor matrix with a larger bandgap. For calculations, we employ the effective mass approximation. It is assumed that the electron and hole of the quantum dot are confined within rectangular potential wells of finite depth.

In the case of the heterostructure crystals under consideration, we assume that the degenerate point of the valence band is the center of the Brillouin zone. We examine semiconductor heterostructures with a sufficiently large spin-orbit interaction, and thus, we do not account for the spin-splitting zone. The energy spectrum of electronic states is determined using the variational Ritz method. The potential energy is chosen in the form of a finite bandgap:

$$U = \begin{cases} 0, & \frac{x^2+y^2}{a^2} + \frac{z^2}{b^2} < 1, \\ U_0, & \frac{x^2+y^2}{a^2} + \frac{z^2}{b^2} \geq 1 , \end{cases}$$

where a and b are the semi-axes of the spheroid, and U_0 is the height of the potential barrier for the charge carrier.

Let's write the Hamiltonian for the electron:

$$\widehat{H} = -\frac{\hbar^2}{2}\nabla\frac{1}{m}\nabla + U, \qquad (1.1)$$

Where

$$m = \begin{cases} m_1, & \frac{x^2+y^2}{a^2} + \frac{z^2}{b^2} < 1, \\ m_2, & \frac{x^2+y^2}{a^2} + \frac{z^2}{b^2} \geq 1 , \end{cases}$$

is the effective mass of the electron for the corresponding region. The Schrödinger equation for a particle with the Hamiltonian (1.1) cannot be solved exactly, so we will perform a transition to new variables. Namely:

$$\tilde{x} = x, \;\; \tilde{y} = y, \;\; \tilde{z} = \frac{a}{b}z.$$

For the new coordinates, we express the Hamiltonian as:

$$\widehat{H} = -\frac{\hbar^2}{2m}\left(\frac{\partial^2}{\partial\tilde{x}^2} + \frac{\partial^2}{\partial\tilde{y}^2}\right) - \frac{\hbar^2}{2m}\frac{a^2}{b^2}\frac{\partial^2}{\partial\tilde{z}^2} + U_{sphere} = -\frac{\hbar^2}{2m}\nabla^2 + U_{sphere} + \frac{\hbar^2}{2m}\left(1 - \frac{a^2}{b^2}\right)\frac{\partial^2}{\partial\tilde{z}^2}, \qquad (1.2)$$

where

$$U_{sphere} = \begin{cases} 0, & \tilde{r} < a, \\ U_0, & \tilde{r} \geq a . \end{cases}$$

We will solve the problem with this Hamiltonian using the variational Ritz method. We choose the trial wave function for the ground state in the form:

$$\Psi(r) = \begin{cases} Cj_0(\tilde{r}ka), & \tilde{r} \leq a, \\ Bh_0^{(1)}(\tilde{r}\chi\beta), & \tilde{r} > a, \end{cases}$$

$$k = \sqrt{\frac{2m_1}{\hbar^2}E}, \quad \chi = \sqrt{\frac{2m_2}{\hbar^2}(E - U_0)}.$$

where $j_0(x)$ is the spherical Bessel function of the first kind, and $h_0^{(1)}(x)$ is the spherical Hankel function of the first kind. By utilizing the continuity conditions of the wave function and probability flux density at the interface of the media, we obtain an expression for determining the coefficients C, B and the dependence $\beta(\alpha) > 0$.

$$B = \frac{2e^{\alpha\chi\beta}\chi\beta\sin[2ka\alpha]}{\sqrt{\pi\alpha\chi\beta + \pi\sin[2ka\alpha]^2 - \frac{\pi\chi\beta\sin[2ka\alpha]}{2ka}}},$$

$$C = \frac{k\sqrt{2\pi}\alpha}{\sqrt{2ka\alpha + \frac{2ka\sin[2ka\alpha]^2}{\chi\beta} - \sin[2ka\alpha]}},$$

$$\beta = -\frac{m_1 - m_2 + km_2\alpha a ctg[ka\alpha]}{m_1\alpha\chi}$$

The dimensions of quantum dots are commensurate with the de Broglie wavelength of the charge carriers, so quantization of charge carrier motion will occur. For the hole, the energy zone will be complex, but in this model of a quantum dot, we can distinguish between heavy and light hole zones. Calculating the energy of size quantization for the ground state of heavy and light holes, it is noteworthy that for heavy holes, it will be significantly smaller, leading to a splitting at the minimum point (Γ-point) of the Brillouin zone between heavy and light hole zones.

Specific calculations were performed for the CdS quantum dot in the SiO_2 matrix. For this nanoheterostructure, the energy of the optical LO-phonon is 57.2 meV. The computation of the energy of the lowest levels of heavy and light holes indicates that the adiabatic approximation can only be applied to quantum dots of small volumes (up to 33 nm), where the distance between the energy levels of heavy and light holes is substantial.

In this work, we will consider small-volume quantum dots, so when investigating interband transitions, we will only take into account the zone of heavy holes.

II. Interaction of Polariton Phonons with Excitons in a Spheroidal Quantum Dot

The equation of motion for the relative displacement vector $\vec{u}$ takes the form:

$$\mu\ddot{\vec{u}} = -\chi\vec{u} + e\vec{E}_{loc}. \quad (2.1)$$

The relationship between the intensity of the local electric field $\vec{E}_{loc}$ and the intensity of the average field $\vec{E}$ and polarization $\vec{P}$ is given by:

$$\vec{E}_{loc} = \vec{E} + \frac{4\pi}{3}\vec{P}, \quad (2.2)$$

and the polarization vector

$$\vec{P} = N\left(e\vec{u} + \alpha\vec{E}_{loc}\right). \quad (2.3)$$

In formulas (2.1)-(2.3), the following notations are introduced:
$\mu = \frac{m_+ m_-}{m_+ + m_-}$ is reduced mass of the ion pair, $\alpha = \alpha_+ + \alpha_-$ is polarizability of this pair, χ is elasticity coefficient, *N* is a number of elementary cells per unit volume of the quantum dot.

The polarization field of the quantum dot is determined by Maxwell's equations for the medium

$$\vec{D} = \varepsilon(\omega)\vec{E} = \vec{E} + 4\pi\vec{P},$$

$$\vec{E} = -\vec{\nabla}\Phi, \quad (2.4)$$

$$div\vec{D} = 0,$$

where $\vec{D}$ is induction vector, Φ is potential of the polarization field. From equations (2.4), we obtain

$$\varepsilon(\omega)\Delta\Phi(\vec{r}) = 0, \quad (2.5)$$

where

$$\varepsilon(\omega) = \varepsilon_\infty \frac{\omega^2 - \omega_L^2}{\omega^2 - \omega_T^2}, \quad (2.6)$$

ε_∞, ω_L, ω_T are known high-frequency dielectric permittivity, frequencies of longitudinal and transverse phonons in a bulk crystal from which the quantum dot is formed.

For confined phonons of the quantum dot:

$$\varepsilon(\omega) = 0, \text{ a } \Delta\Phi(\vec{r}) \neq 0. \quad (2.7)$$

Therefore, as seen from (2.6), the frequency of confined oscillations of polarization coincides with the frequency of longitudinal optical oscillations $\omega = \omega_L$.

Now let's determine the potential of the polarization field $\Phi_L(\vec{r})$ and the corresponding component of the displacement vector $\vec{u}_L$, caused by confined optical phonons. Since $\varepsilon(\omega) = 0$, then from the first equation (2.4) we have:

$$\vec{E} = -4\pi\vec{P}_L. \quad (2.8)$$

where the index *L* indicates that the longitudinal component is considered. Substituting (2.8) into equation (2.2), we obtain a relationship between the local field and polarization:

$$\vec{E}_{loc} = -\frac{8\pi}{3}\vec{P}_L. \quad (2.9)$$

From equations (2.3) and (2.9), we find the polarization vector in the form:

$$\vec{P}_L = \frac{Ne}{1+2\beta}\vec{u}_L, \quad (2.10)$$

where $\beta = \frac{4}{3}\pi Na$. Returning again to equations (2.4), where we have the equation for the potential $\Phi_L(\vec{r})$. Taking into account the conditions (2.8) and (2.10), we have that:

$$\Delta\Phi_L(\vec{r}) = \frac{4\pi Ne}{1+2\beta}\vec{u}_L(\vec{r}). \quad (2.11)$$

When searching for the potential, it is necessary to take into account that the polarization corresponding to confined phonons disappears at the surface of the quantum dot

$$\Phi_L(\vec{r})|_S = 0. \quad (2.12)$$

Let's consider the case of an elongated spheroid.

The elongated spheroidal coordinates ξ, η, ϕ related to the rectangular coordinates of the point x, y, z by the following formulas:

$$x = \frac{d}{2}\sqrt{(\xi^2 - 1)(1 - \eta^2)}\cos\phi,$$

$$y = \frac{d}{2}\sqrt{(\xi^2 - 1)(1 - \eta^2)}\sin\phi,$$

$$z = \frac{d}{2}\xi\eta,$$

$\xi \in [1, \infty]$, $\eta \in [-1, 1]$, $\phi \in [0, 2\pi]$, $\frac{d}{2}$ – focal length. The volume element computed using the Lame coefficients takes the form

$$dV = dxdydz = \frac{d^3}{8}(\xi^2 - \eta^2)d\xi d\eta d\phi. \quad (2.13)$$

The Laplace operator in elongated spheroidal coordinates is equal to

$$\nabla^2 = \Delta = \frac{4}{d^2(\xi^2 - \eta^2)}\left\{\frac{\partial}{\partial\xi}(\xi^2 - 1)\frac{\partial}{\partial\xi} + \frac{\partial}{\partial\eta}(1 - \eta^2)\frac{\partial}{\partial\eta} + \frac{\xi^2 - \eta^2}{(\xi^2 - 1)(1 - \eta^2)}\frac{\partial^2}{\partial\phi^2}\right\}. \quad (2.14)$$

The Helmholtz equation for the potential is given by:

$$(\Delta + k^2)\Phi_L(\vec{r}) = 0, \tag{2.15}$$

where k is wave number.

If the potential $\Phi_L(\vec{r})$ is expressed as the product:

$$\Phi_L(\vec{r}) = R_{ml}(\xi)S_{ml}(\eta)e^{\pm im\phi}, \quad m=0, 1, 2, \tag{2.16}$$

then the Helmholtz equation allows for variable separation. Thus, for the functions $R_{ml}(\xi)$, $S_{ml}(\eta)$ we obtain ordinary differential equations:

$$\frac{\partial}{\partial\xi}\left[(\xi^2-1)\frac{\partial}{\partial\xi}R_{ml}(\xi)\right] + \left[-\lambda_{ml} + c^2(\xi^2-1) - \frac{m^2}{\xi^2-1}R_{ml}(\xi)\right] = 0, \tag{2.17}$$

$$\frac{\partial}{\partial\eta}\left[(1-\eta^2)\frac{\partial}{\partial\eta}S_{ml}(\eta)\right] + \left[\lambda_{ml} + c^2(1-\eta^2) - \frac{m^2}{1-\eta^2}S_{ml}(\eta)\right] = 0, \tag{2.18}$$

Where $c = \frac{kd}{2} \geq 0$, λ_{ml} is separation constant, m is integer.

The solutions to equations (2.17), (2.18) will be denoted as $R_{ml}(\xi)$ – elongated radial and $S_{ml}(\eta)$ – elongated spherical angular functions (ESAF) [15].

We return to equation (2.11). The potential $\Phi_L(\vec{r})$ will be sought in the form of an expansion over the complete set of ESAF functions:

$$\Phi_L(\vec{r}) = \sum_{lmn} A_{lmn}R_{ml}(c_n,\xi)\,S_{ml}(c_n\eta)e^{im\phi}. \tag{2.22}$$

Using (2.22), the displacement in (2.11) can be written as:

$$\vec{u}_L(\vec{r}) = \sum_{lmn}\vec{U}_{lmn}, \tag{2.23}$$

where

$$\vec{U}_{lmn} = \left(\frac{1+2\beta}{4\pi ne}\right)A_{lmn}\vec{\nabla}\left(R_{ml}(c_n,\xi)S_{ml}(c_n,\eta)e^{im\phi}\right) \tag{2.24}$$

The coefficients A_{lmn} remain unknown. We will determine them in the process of the secondary quantization of the phonon field.

To do this, it is necessary to write the equation of motion for $\vec{u}_L$, characterized by the effective mass of ions μ and the frequency of longitudinal ω_L.

$$\ddot{\vec{u}}_L = -\omega_L^2\vec{u}_L. \tag{2.25}$$

To obtain equation (2.25), it is necessary to introduce the Lagrangian density in the form of

$$L = T - V - \frac{n\mu}{2}\left(\dot{\vec{u}}_L^2 - \omega^2\vec{u}_L^2\right). \tag{2.26}$$

Then the density of the generalized momentum is equal to:

$$\frac{\partial L}{\partial\dot{\vec{u}}_L} \equiv \vec{p}_L = N\mu\dot{\vec{u}}_L. \tag{2.27}$$

Now we can write the Hamiltonian function for confined polar phonon oscillations of the quantum dot:

$$H = \int_V \left(\frac{p_L^2}{2n\mu} + \frac{1}{2}N\mu\omega_L^2u_L^2\right)dV. \tag{2.28}$$

Let's proceed to the operators of physical quantities, following the principles of quantum mechanics:

$$\vec{p}_L \to \hat{\vec{p}}_L, \quad \vec{u}_L \to \hat{\vec{u}}_L, \tag{2.29}$$

Similarly to classical relationships

$$\hat{\vec{p}}_L = \sum_{lmn}\hat{\vec{P}}_{lmn}, \hat{\vec{u}}_L = \sum_{lmn}\hat{\vec{U}}_{lmn}, \tag{2.30}$$

We need to transition from canonical variables to operators of second quantization b_{lmn}, b_{lmn}^+, that would satisfy bosonic commutation relations:

$$\left[\hat{b}_{lmn}, \hat{b}^+_{lm'n'}\right] = \delta_{ll}\cdot\delta_{mm}\cdot\delta_{nn}. \tag{2.31}$$

Let's express the operators in the form

$$\hat{\vec{U}}_{lmn} = A_{lmn}\sqrt{\frac{\hbar}{2N\mu\omega_L}}\vec{\nabla}\left[R_{ml}(c_n,\xi)S_{ml}(c_n,\eta)e^{im\phi}\right](b^+_{lmn} + b_{lmn}), \tag{2.32}$$

$$\hat{\vec{P}}_{lmn} = A_{lmn}\sqrt{\frac{\hbar N\mu\omega_L}{2}}\vec{\nabla}\left[R_{ml}(c_n,\xi)S_{ml}(c_n,\eta)e^{-im\phi}\right](b^+_{lmn} - b_{lmn}). \tag{2.33}$$

The Hamiltonian of polarization oscillations

$$\widehat{H}_L = \frac{1}{2}\int dV\left(\frac{\hat{\vec{P}}_L^{+}\hat{\vec{P}}_L}{N\mu} + N\mu\omega_L^2\hat{\vec{U}}_L^{+}\hat{\vec{U}}_L\right) =$$
$$\sum_{\substack{lmn\\ l'm'n'}} \frac{\hbar\omega_L}{4} A^*_{lmn}A_{l'm'n'} \int \nabla\left[R_{ml}(c_n,\xi)S_{ml}(c_n,\eta)e^{-im\phi}\right]\times\nabla\left[R_{m'l'}(c_{n'},\xi)S_{m'l'}(c_{n'},\eta)e^{im'\phi}\right]\{(b_{lmn}-b^+_{lmn})\times$$
$$\left(b^+_{l'm'n'}-b_{l'm'n'}\right)+(b^+_{lmn}+b_{lmn})\times\left(b_{l'm'n'}+b^+_{l'm'n'}\right)\}dV =$$
$$\sum_{\substack{lmn\\ l'm'n'}} A^*_{lmn}A_{l'm'n'}\int\nabla\left[R_{ml}(c_n,\xi)S_{ml}(c_n,\eta)e^{-im\phi}\right]\times\nabla\left[R_{m'l'}(c_{n'},\xi)S_{m'l'}(c_{n'},\eta)e^{im'\phi}\right]dV\times\left[\hbar\omega\left(b^+_{lmn}b_{lmn}+\frac{1}{2}\right)\right]. \quad (2.34)$$

The volume integral over the quantum dot is calculated using Green's theorem. Taking into account that the potential on the surface is zero (2.12), therefore, according to (2.22) $R_{ml}(c_n,\xi_0)=0$, because $\xi=\xi_0$ determines the surface of the spheroid. So,

$$\int_V dV\nabla\left[R_{ml}(c_n,\xi)S_{ml}(c_n,\eta)e^{-im\phi}\right]\nabla\left[R_{m'l'}(c_{n'},\xi)S_{m'l'}(c_{n'},\eta)e^{im'\phi}\right] =$$
$$-\int_V dV\left(R_{ml}(c_n,\xi)S_{ml}(c_n,\eta)e^{-im\phi}\right)\nabla^2\left(R_{m'l'}(c_{n'},\xi)S_{m'l'}(c_{n'},\eta)e^{im'\phi}\right). \quad (2.35)$$

Let's recall that

$$dV=\frac{d^3}{8}(\xi^2-\eta^2)\,d\xi d\eta d\phi, \quad (2.36)$$

$$\nabla^2=\frac{4}{d^2(\xi^2-\eta^2)}\left\{\frac{\partial}{\partial\xi}(\xi^2-1)\frac{\partial}{\partial\xi}+\frac{\partial}{\partial\eta}(1-\eta^2)\frac{\partial}{\partial\eta}+\frac{\xi^2-\eta^2}{(\xi^2-1)(1-\eta^2)\,\partial\phi^2}\right\}. \quad (2.37)$$

Let's compute the integral (2.35). Taking into account (2.36) and (2.37), we obtain:

$$I=-\frac{d}{2}\int d\xi d\eta d\phi\left(R_{ml}(c_n,\xi)S_{ml}(c_n,\eta)e^{-im\phi}\right)\times\left\{\frac{\partial}{\partial\xi}(\xi^2-1)\frac{\partial}{\partial\xi}+\frac{\partial}{\partial\eta}(1-\eta^2)\frac{\partial}{\partial\eta}+\frac{\xi^2-\eta^2}{(\xi^2-1)(1-\eta^2)\,\partial\phi^2}\right\}\times$$
$$\left(R_{m'l'}(c_{n'},\xi)S_{m'l'}(c_{n'},\eta)e^{im'\phi}\right)=-\frac{d}{2}\int d\xi d\eta d\phi\, R_{ml}(c_n,\xi)S_{ml}(c_n,\eta)e^{-im\phi}\times\left\{\frac{\partial}{\partial\xi}(\xi^2-1)\frac{\partial}{\partial\xi}+\frac{\partial}{\partial\eta}(1-\eta^2)\frac{\partial}{\partial\eta}+\right.$$
$$\left.\frac{\xi^2-\eta^2}{(\xi^2-1)(1-\eta^2)\,\partial\phi^2}\right\}\times R_{m'l'}(c_{n'},\xi)S_{m'l'}(c_{n'},\eta)e^{im'\phi}.$$

Taking into account that

$$\int_0^{2\pi}e^{i(m'-m)\varphi}=2\pi\delta_{mm'},$$

Then, the reduced integral *I* reduces to the following:

$$I=-\pi d\delta_{mm'}\int d\,\xi d\eta R_{ml}(c_n,\xi)S_{ml}(c_n,\eta)\times$$
$$\times\left\{\frac{\partial}{\partial\xi}(\xi^2-1)\frac{\partial}{\partial\xi}+\frac{\partial}{\partial\eta}(1-\eta^2)\frac{\partial}{\partial\eta}-\frac{m^2}{\xi^2-1}-\frac{m^2}{1-\eta^2}\right\}R_{m'l'}(c_{n'},\xi)S_{m'l'}(c_{n'},\eta). \quad (2.38)$$

Now, taking into account equations (2.17) and (2.18), we have

$$I=-\pi d\delta_{mm'}\int d\,\xi d\eta R_{ml}(c_n,\xi)S_{ml}(c_n,\eta)\left\{\left(\lambda-c^2(\xi^2-1)\right)+\left(-\lambda-c^2(1-\eta^2)\right)\right\}\times R_{m'l'}(c_{n'},\xi)S_{m'l'}(c_{n'},\eta)=$$
$$\pi dc_n^2\delta_{mm'}\delta_{ll'}\delta_{nn'}\left\{\int_1^{\xi_0}d\xi R^2_{ml}(c_n,\xi)\,\xi^2-\int_{-1}^{1}d\eta S^2_{ml}(c_n,\eta)\eta^2\right\}. \quad (2.39)$$

$$\widehat{H}=\sum_{lmn}\hbar\omega_L\left(b^+_{lmn}b_{l'm'n'}+\frac{1}{2}\right)\delta_{mm'}\delta_{ll'}\delta_{nn'}|A_{lmn}|^2\pi dc_n^2\left[\int_1^{\xi_0}d\xi R^2_{ml}(c_n,\xi)\,\xi^2-\int_{-1}^{1}d\eta S^2_{ml}(c_n,\eta)\eta^2\right]=$$
$$\sum_{lmn}\hbar\omega_L\left(b^+_{lmn}b_{lmn}+\frac{1}{2}\right), \quad (2.40)$$

if

$$A_{lmn}=\left\{\pi dc_n^2\left[\int_1^{\xi_0}d\xi R^2_{ml}(c_n,\xi)\,\xi^2-\int_{-1}^{1}d\eta S^2_{ml}(c_n,\eta)\eta^2\right]\right\}^{-\frac{1}{2}}=\frac{1}{\sqrt{\pi d}}\cdot\frac{1}{c_n}\cdot\frac{1}{\sqrt{\int_1^{\xi_0}d\xi R^2_{ml}(c_n,\xi)\xi^2-\int_{-1}^{1}d\eta S^2_{ml}(c_n,\eta)\eta^2}} \quad (2.41)$$

Substituting $\hat{U}_{lmn}$ the formula (2.32) into the formula (2.11), assuming that the potential Φ is an operator. Therefore,

$$\widehat{\Phi}=\frac{4\pi ne}{1+2\beta}A_{lmn}\sqrt{\frac{\hbar}{2n\mu\omega_L}}R_{ml}(c_n,\xi)S_{ml}(c_n,\eta)e^{im\phi}(b^+_{lmn}+b_{lmn}). \quad (2.42)$$

Taking into account that

$$\frac{1}{1+2\beta}\sqrt{\frac{4\pi ne^2}{\mu\omega_L^2}}=\sqrt{\frac{1}{\varepsilon_\infty}-\frac{1}{\varepsilon_0}}. \tag{2.43}$$

Then the potential operator

$$\widehat{\Phi}=\sqrt{2\pi\hbar\omega_L}\sqrt{\frac{1}{\varepsilon_\infty}-\frac{1}{\varepsilon_0}}\cdot\frac{1}{\sqrt{\pi d}}\frac{1}{C_n}\left[\frac{\int_1^{\xi_0}d\xi R_{ml}^2(c_n,\xi)\,\xi^2}{\int_1^{\xi_0}d\xi R_{ml}^2(c_n,\xi)}-\frac{\int_{-1}^{1}d\eta S_{ml}^2(c_n,\eta)\eta^2}{\int_{-1}^{1}d\eta S_{ml}^2(c_n,\eta)}\right]^{\frac{1}{2}}\times$$
$$\times\frac{R_{ml}(c_n,\xi)}{\sqrt{\int_1^{\xi_0}d\xi R_{ml}^2(c_n,\xi)}}-\frac{S_{ml}(c_n,\eta)}{\sqrt{\int_{-1}^{1}d\eta S_{ml}^2(c_n,\eta)}}e^{im\phi}(b_{lmn}^{+}+b_{lmn}). \tag{2.44}$$

And the electron-phonon interaction operator will take the form:

$$\widehat{H}_{int}=-e\widehat{\Phi}=-e\sqrt{\frac{2\hbar\omega_L}{d}}\sqrt{\frac{1}{\varepsilon_\infty}-\frac{1}{\varepsilon_0}}\cdot\frac{1}{C_n}\left[\frac{\int_1^{\xi_0}d\xi R_{ml}^2(c_n,\xi)\xi^2}{\int_1^{\xi_0}d\xi R_{ml}^2(c_n,\xi)}-\frac{\int_{-1}^{1}d\eta S_{ml}^2(c_n,\eta)\eta^2}{\int_{-1}^{1}d\eta S_{ml}^2(c_n,\eta)}\right]^{\frac{1}{2}}\times$$
$$\times\frac{R_{ml}(c_n,\xi)}{\sqrt{\int_1^{\xi_0}d\xi R_{ml}^2(c_n,\xi)}}-\frac{S_{ml}(c_n,\eta)}{\sqrt{\int_{-1}^{1}d\eta S_{ml}^2(c_n,\eta)}}e^{im\phi}(b_{lmn}^{+}+b_{lmn}). \tag{2.45}$$

Let's write down the exciton-phonon interaction function, taking into account spontaneous phonon emission [16], we get:

$$\widehat{\Phi}_0(m,l,n)=\int_1^{\xi_0}d\xi_e\int_{-1}^{1}d\eta_e\int_0^{2\pi}d\phi_e\varphi_e^*(\xi_e,\eta_e,\phi_e)\int_1^{\xi_0}d\xi_h\int_{-1}^{1}d\eta_h\int_0^{2\pi}d\phi_h\varphi_h^*(\xi_h,\eta_h,\phi_h)\big(e\widehat{\Phi}_h-$$
$$e\widehat{\Phi}_e\big)\varphi_e(\xi_e,\eta_e,\phi_e)\,\varphi_h(\xi_h,\eta_h,\phi_h)=$$
$$\int_1^{\xi_0}d\xi_e\int_{-1}^{1}d\eta_e\int_0^{2\pi}d\phi_e\varphi_e^2(\xi_e,\eta_e,\phi_e)\int_1^{\xi_0}d\xi_h\int_{-1}^{1}d\eta_h\int_0^{2\pi}d\phi_h\varphi_h^2(\xi_h,\eta_h,\phi_h)\big(e^{im\phi_h}F_h-e^{im\phi_e}F_e\big), \tag{2.46}$$

where $\varphi_e(\xi_e,\eta_e,\phi_e)$, $\varphi_h(\xi_h,\eta_h,\phi_h)$ the wave functions of the electron and hole, respectively.

$$F=e\sqrt{\frac{2\hbar\omega_L}{d}}\sqrt{\frac{1}{\varepsilon_\infty}-\frac{1}{\varepsilon_0}}\cdot\frac{1}{C_n}\left[\frac{\int_1^{\xi_0}d\xi R_{ml}^2(c_n,\xi)\xi^2}{\int_1^{\xi_0}d\xi R_{ml}^2(c_n,\xi)}-\frac{\int_{-1}^{1}d\eta S_{ml}^2(c_n,\eta)\eta^2}{\int_{-1}^{1}d\eta S_{ml}^2(c_n,\eta)}\right]^{\frac{1}{2}}\times\frac{R_{ml}(c_n,\xi)}{\sqrt{\int_1^{\xi_0}d\xi R_{ml}^2(c_n,\xi)}}\frac{S_{ml}(c_n,\eta)}{\sqrt{\int_{-1}^{1}d\eta S_{ml}^2(c_n,\eta)}}. \tag{2.47}$$

Taking into account that $m_e=m_h=0$, $e^{im\phi_h}=e^{im\phi_e}=1$ і $\varphi_e(\xi_e,\eta_e,\phi_e)=\varphi_e(\xi_e,\eta_e)$, $\varphi_h(\xi_h,\eta_h,\phi_h)=\varphi_h(\xi_h,\eta_h)$, simplify (2.46) as follows:

$$\widehat{\Phi}_0(m,l,n)=\int_1^{\xi_0}d\xi_e\int_{-1}^{1}d\eta_e\int_0^{2\pi}d\phi_e\varphi_e^2(\xi_e,\eta_e)\int_1^{\xi_0}d\xi_h\int_{-1}^{1}d\eta_h\int_0^{2\pi}d\phi_h\,e^{im\phi_h}\varphi_h^2(\xi_h,\eta_h)F_h-$$
$$\int_1^{\xi_0}d\xi_e\int_{-1}^{1}d\eta_e\int_0^{2\pi}d\phi_e e^{im\phi_e}\varphi_e^2(\xi_e,\eta_e)\int_1^{\xi_0}d\xi_h\int_{-1}^{1}d\eta_h\int_0^{2\pi}d\phi_h\varphi_h^2(\xi_h,\eta_h)F_e=$$
$$(2\pi)^2\int_1^{\xi_0}d\xi_e\int_{-1}^{1}d\eta_e\varphi_e^2(\xi_e,\eta_e)\int_1^{\xi_0}d\xi_h\int_{-1}^{1}d\eta_h\varphi_h^2(\xi_h,\eta_h)F_h=$$
$$(2\pi)^2\int_1^{\xi_0}d\xi_e\int_{-1}^{1}d\eta_e\varphi_e^2(\xi_e,\eta_e)\int_1^{\xi_0}d\xi_h\int_{-1}^{1}d\eta_h\varphi_h^2(\xi_h,\eta_h)F_e \tag{2.48}$$

The coefficient of interband light absorption is found using the formula:

$$\alpha(\omega)=\frac{4\pi^2e^2}{ncm_0^2\hbar\omega V_0}D_{ex}\,\mathrm{Im}[G_n(\widetilde{\omega})] \tag{2.49}$$

where $G_n(\widetilde{\omega})=-\frac{i}{\hbar}\cdot e^{-g_0}\cdot g_n(\omega)$ is Green's function, $g_n(\omega)=\int_0^{\infty}e^{-\eta t}\cdot e^{i(\omega-\omega_n)t}\cdot e^{\sum_m^M|\Lambda_{mn}|^2[(1+\tilde{V}_m)e^{-i\omega f_m t}+\tilde{V}_m e^{i\omega f_m t}]}d$, $g_0=\sum_m^M|\Lambda_{m0}|^2\big(2\tilde{V}_m+1\big)$, $\tilde{V}_l=\frac{1}{e^{\frac{\Omega^l}{k_bT}}}$, $\Lambda_{mn}=\sum_l\frac{\widetilde{\Phi}_0(m,l,n)}{\Omega_L}$, m,l,n are phonon quantum numbers, $\Omega_L=\hbar\omega_L$ is the energy of confined phonons.

III. Interband Light Absorption in Heterostructures

We consider the interband light absorption in a semiconductor quasi-zero-dimensional nanoheterosystem based on the dipole approximation, as the electromagnetic wave's wavelength is significantly larger than the quantum dot dimensions.

In practice, ensembles of quantum dots (QDs) are often obtained within crystalline or polymeric matrices or in colloidal solutions. Regardless of the growth method used, the set of QDs is always characterized by size dispersion. It is assumed that the distribution of QDs by

size can be approximated by a Gaussian function. Using formula (2.49), dependencies of the coefficient of electromagnetic wave absorption on the incident quantum energy are plotted for an average QD volume of 14 nm³ and a size dispersion of 1%. For each dependency, we denote the coefficient K, representing the ratio of the major (b) to minor (a) axes of the ellipsoid.

Figure 1 shows the absorption coefficient obtained for a quantum dot of an elongated spheroid shape. In the energy transition range, there are four absorption peaks: two of them are due to charge carrier transitions between optically active levels in the quantum dot (phonon-free bands), and the other two arise from electron-phonon interactions and are phonon replicas. In this figure, the graphs of the light interband absorption coefficient as a function of the frequency of the incident electromagnetic wave for both the interaction of excitons with confined phonons and the bulk model practically coincide. This occurs due to the relationship of the ellipsoid semi-axes K = 1.01, which means that $b \approx a$. The calculations show that the magnitude of the exciton-phonon interaction in the model of such a quasi-sphere is almost independent of the choice of phonons involved in the interband light absorption.

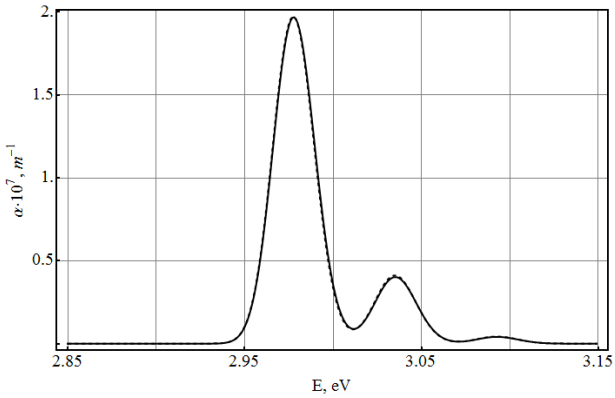

Fig. 1. Interband absorption coefficients considering confined phonons (solid curve), T = 4.2 K, K = 1.01. The dashed curve corresponds to $\alpha = \alpha(\omega)$ absorption considering phonons of the bulk crystal.

When studying the absorption coefficients of interband optical transitions, an important factor is the temperature at which the transition occurs. In Fig. 2, the light absorption coefficient for interband transitions of charge carriers is shown for the same models of a quantum dot in the form of an elongated ellipsoid of revolution at room temperature (T = 300 K). Comparing the shape of the absorption coefficient frequency dependence graph with the graph in Fig. 1 (T = 4.2 K), we note the appearance of additional phonon replicas to the left of the non-phonon maxima of the absorption coefficient. The absolute values of the absorption coefficient maxima for all transitions have slightly decreased.

Let's analyze Fig. 3 in more detail. The considered QD model is a spheroid with an aspect ratio of 0.5, meaning $b = 1.5a$. We observe that for both cases (considering confined phonons as well as phonons of the bulk crystal), light absorption occurs at approximately the same energies. However, compared to the "quasisphere" case (Figures 1 and 2), the overall energy at which light

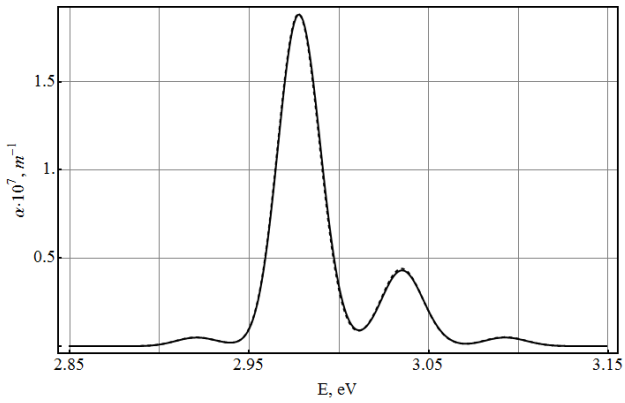

Fig. 2. Interband absorption coefficients considering confined phonons (solid curve), T = 300 K, K = 1.01. The dashed curve corresponds to $\alpha = \alpha(\omega)$ absorption considering phonons of the bulk crystal.

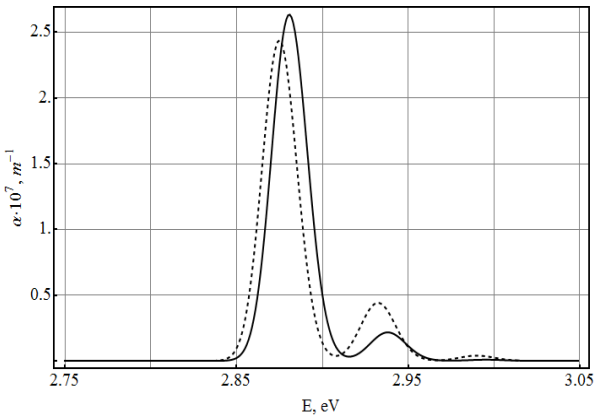

Fig. 3. Interband absorption coefficients taking into account confined phonons (solid curve), T = 4.2 K, K = 1.5. The dashed curve corresponds to $\alpha = \alpha(\omega)$ absorption considering phonons of the bulk crystal.

absorption occurs decreases - the absorption wavelength shifts towards the red part of the spectrum. It is evident that the absorption peaks considering confined phonons are shifted towards higher energies compared to the case considering bulk phonons. The absolute values of the absorption coefficient maxima, which are caused by phonon replicas, are higher for the model with bulk phonons, except for light absorption during the charge transition between the lowest (ground) states of the electron and hole, where the maximum of the interband light absorption coefficient with confined phonons is higher.

When comparing the contribution of confined phonon polarizations with bulk phonons to the interband charge transition process under the influence of external electromagnetic waves, we observe that the difference in absolute values of absorption peaks in Fig. 4 increases for all absorption maxima due to the temperature rise to 300 K.

Comparing the transitions driven by exciton-phonon interaction, namely interband optical transitions with confined phonons and bulk phonons, we observe that the phonon replicas play a more significant role in the maxima of light optical absorption, especially for the case of bulk phonons, across the entire absorption range at the considered temperatures.

Examining Figures 5-6, which depict absorption spectra for quantum dots in the form of an elongated spheroid with an aspect ratio of K=2 ($b = 2a$), we observe

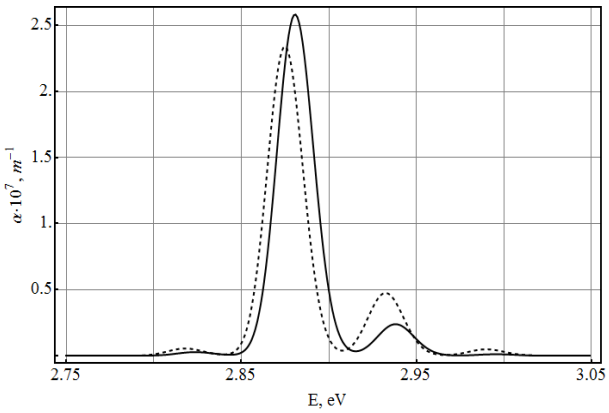

Fig. 4. Interband absorption coefficients taking into account confined phonons (solid curve), T = 300 K, K = 1.5. The dashed curve corresponds to $\alpha = \alpha(\omega)$ absorption considering phonons of the bulk crystal.

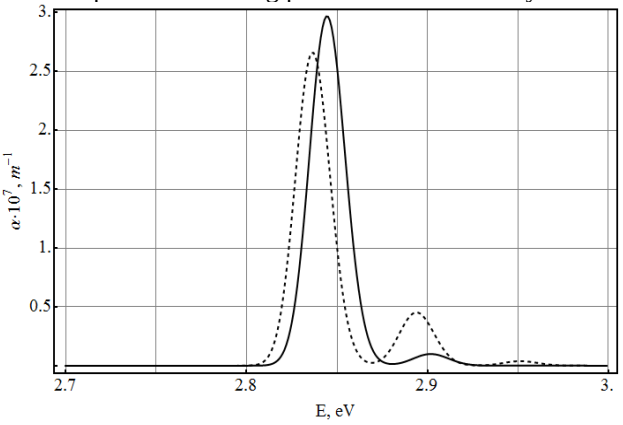

Fig. 5. Interband absorption coefficients taking into account confined phonons (solid curve), T = 4.2 K, K = 2. The dashed curve corresponds to $\alpha = \alpha(\omega)$ absorption considering phonons of the bulk crystal.

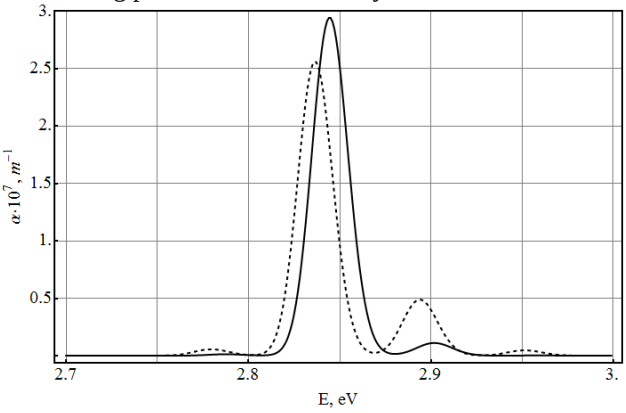

Fig. 6. Interband absorption coefficients taking into account confined phonons (solid curve), T = 300 K, K = 2. The dashed curve corresponds to $\alpha = \alpha(\omega)$ absorption considering phonons of the bulk crystal.

an increase in the absolute values of the absorption coefficient maxima between the two lowest optically active electron and hole levels (phonon-free absorption band). This difference from models with a smaller aspect ratio is explained by a reduction in the probability of interband charge carrier transitions due to the interaction with phonons resulting from light absorption.

Analyzing the plots of the dependence of the interband light absorption coefficient on the frequency of the incident electromagnetic wave in Figures 5-6, we observe even more "smoothing" of phonon replicas across the entire absorption range when considering polariton-confined phonons. It is noteworthy that when considering exciton-phonon interaction in the bulk model, the absolute values of the absorption maxima of phonon replicas are significantly higher than the peak values calculated with confined phonons in the quantum dot.

Further increasing the aspect ratio of the quantum dot in the form of an elongated spheroid, in our opinion, will simultaneously result in a narrowing of the region where interband charge carrier transitions occur, accompanied by a reduction in the distances between levels.

It is visually evident that at large aspect ratios of the ellipsoidal-shaped quantum dot CdS/SiO_2 the interaction of charge carriers with confined phonons diminishes, and the non-phonon absorption bands will have a much higher probability of interband transitions for the charge carriers than the phonon replicas.

Conclusions

In this study, we have investigated the interband absorption spectrum of CdS quantum dots with a spherical shape embedded in a SiO2 matrix, taking into account the interaction of electron-hole pairs with polariton phonons. We analyzed the differences between the volume Fröhlich model (phonons of a bulk crystal) and the interaction of the exciton-phonon system, considering confined phonons. Absorption coefficients related to charge carrier transitions between the lowest excitonic optically active levels in quantum dots under the influence of linearly polarized light were calculated. We focused on quantum dot volumes where the energy levels of electrons and holes are sufficiently separated. Thus, considering the possible dispersion of quantum dots in size within the matrix and accounting for different aspect ratios for quantum dots with an elongated spheroid shape, the identified levels can be distinguished in the analysis of the frequency dependence of the interband absorption coefficient. The calculations demonstrate that both the peak magnitudes and the energies of the interband absorption coefficient peaks depend not only on the volume and shape of quantum dots but also on the choice of the phonon model. For this heterostructure, we have shown the similarity of absorption spectra when considering both bulk crystal phonons and confined phonons.

Holskyi V.B. – Candidate of Physical and Mathematical Sciences, Associate Professor of the Department of Physics and Information Systems;
Leshko R.Ya. – Candidate of Physical and Mathematical Sciences, Associate Professor of the Department of Physics and Information Systems;
Brytan V.B. – Candidate of Physical and Mathematical Sciences, Associate Professor of the Department of Physics and Information Systems;
Uhryn Y.O. – Candidate of Physical and Mathematical Sciences, Associate Professor of the Department of Physics and Information Systems;
Karpiy V.R. – graduate student of the Department of Physics and Information Systems.

[1] D.V. Korbutyak, O.V. Kovalenko, S.I. Budzulyak, S.M. Kalitchuk, I.M. Kupchak, *Light-Emitting Properties of A_2B_6 Semiconductor Quantum Dots*, Ukr. Phys. J. Reviews, 7 (1), 48 (2012).
[2] Y. Yakar, B. Cakır, A. Ozmen, *Calculation of Linear and Nonlinear Optical Absorption Coefficients of a Spherical Quantum Dot with Parabolic Potentia*, Optics Communications 283, 1795 (2010); http://dx.doi.org/10.1016/j.optcom.2009.12.027.
[3] M.R.K. Vahdani, G. Rezaei, *Linear and nonlinear optical properties of a hydrogenic donor in lens-shaped quantum dots*, Phys. Lett. A, 373, 3079 (2009); https://doi.org/10.1016/j.physleta.2009.06.042..
[4] G. Cantele, D. Ninno and G. Iadonisi, *Calculation of the Infrared Optical Transitions in Semiconductor Ellipsoidal Quantum Dots*, Nano Letters 1, 121 (2001); https://doi.org/10.1021/nl0055310,
[5] L.E. Vorob'ev, V.Y. Panevin, N.K. Fedosov, et al., *Optical phenomena in InAs/GaAs heterostructures with doped quantum dots and artificial molecules*. Semiconductors 39, 50 (2005); https://doi.org/10.1134/1.1852644.
[6] T.O. Cheche, M.C. Chang b, S.H. Lin, *Electron–phonon interaction in absorption and photoluminescence spectra of quantum dots*, Chemical Physics. 309, 109 (2005); https://doi.org/10.1016/j.chemphys.2004.08.018.
[7] V.I. Boichuk, I.V. Bilynsky, I.O. Shakleina, *Energy spectrum of a charge of quantum dots with different shapes*, Ukr. J. Phys. 53, 894 (2008).
[8] Sergio Bietti, Juanita Bocquel, Silvia Adorno, Takaaki Mano, Joris G. Keizer, Paul M. Koenraad, and Stefano Sanguinetti, *Precise shape engineering of epitaxial quantum dots by growth kinetics*, Phys. Rev. B, 92, 075425 (2015); https://doi.org/10.1103/PhysRevB.92.075425.
[9] J.H. Blokland, M. Bozkurt, J.M. Ulloa, D. Reuter, A.D. Wieck, P.M. Koenraad, P.C.M. Christianen and J.C. Maan, *Ellipsoidal InAs quantum dots observed by cross-sectional scanning tunneling microscopy*, Applied Physics Letters, 94, 023107 (2009); https://doi.org/10.1063/1.3072366.
[10] V. Kladko, M. Slobodian, P. Lytvyn, V. Strelchuk, Yu. Mazur, E. Marega, M. Hussein and G. Salamo, *Three-dimensional ordering in self-organized (In,Ga)As quantum dot multilayer structures*, Phys. Status Solidi A, 206, 1748 (2009); https://doi.org/10.1002/pssa.200881593.
[11] F Comas, C Trallero-Giner, N Studart and G E Marques, *Interface optical phonons in spheroidal quantum dots*, J. Phys.: Condens. Matter, 14, 6469 (2002); https://doi.org/10.1088/0953-8984/14/25/314.
[12] F. Comas, C. Trallero-Giner, Nelson Studart, and G. E. Marques, *Interface optical phonons in spheroidal dots: Raman selection rules*, Physical Review B, 65, 073303 (2002); https://doi.org/10.1103/PhysRevB.65.073303.
[13] L. Shi, Z.W. Yan, *Bound polaron in a wurtzite nitride semiconductor ellipsoidal quantum dot*, Physica E, 41, 1353 (2009); https://doi.org/10.1016/j.physe.2009.03.012.
[14] A.M. Alcalde, A.A. Ribeiro, N.O. Dantas, D.R. Mendes Jr., G.E. Marques, C. Trallero-Giner, *Optical phonons and Raman scattering in ternary II–VI spheroidal nanocrystals embedded in a glass matrix*, Journal of Non-Crystalline Solids, 352, 3618 (2006); https://doi.org/10.1016/j.jnoncrysol.2006.03.109.
[15] Le-Wei Li, Xiao-Kang Kang, Mook-Seng, Leong Spheroidal Wave Functions in Electromagnetic Theory (New York, 2002).
[16] H. Fehske, A. Alvermann, M. Hohenadler, and G. Wellein, in Polarons in Bulk Materials and Systems with Reduced Dimensionality, Proc. Int. School of Physics "Enrico Fermi", Course CLXI, edited by G. Iadonisi, J. Ranninger, and G. De Filippis (IOS Press, Amsterdam, Oxford, Tokio, Washington DC, 2006)

В.Б. Гольський, Р.Я. Лешко, В.Б. Британ, Ю.О. Угрин, В.Р. Карпій

Вплив поляризаційних фононів на міжзонне поглинання світла у сфероїдальній квантовій точці гетеросиситеми CdS/SiO_2

Дрогобицький державний педагогічний університет імені Івана Франка,
факультет фізики, математики, економіки та інноваційних технологій, кафедра фізики та інформаційних систем,
м. Дрогобич, Україна, hol.wit@gmail.com

Досліджено вплив обмежених фононів на коефіцієнт міжзонного поглинання поляризованого світла від його частоти. Зроблено порівняння отриманих результатів із відповідними при врахуванні поляризаційних фононів масивного кристалу. Встановлено залежність міжзонного поглинання світла від співвідношення півосей еліпсоїда. Обчислення проводились для різних температур і радіусів квантової точки гетероструктури CdS/SiO_2 форми витягнутого сфероїда.

Ключові слова: фактор Хуанга-Ріса, оптичні переходи, фонони, коефіцієнт поглинання.